ORNL/SPR-2024/3575

Light Water Reactor Sustainability Program

Complete the Second Weld Campaign on Ni Alloy 182 Using Optimized Welding Parameters and Complete the Initial Weld Quality Evaluation

M2LW-24OR0406013

September 2024
U.S. Department of Energy
Office of Nuclear Energy

ORNL/SPR-2024/3575

Materials Science and Technology Division

COMPLETE THE SECOND WELD CAMPAIGN ON NI ALLOY 182 USING OPTIMIZED WELDING PARAMETERS AND COMPLETE THE INITIAL WELD QUALITY EVALUATION

M2LW-24OR0406013

Jian Chen, Roger Miller, Zhili Feng
Oak Ridge National Laboratory

Jonathan Tatman, Benjamin Sutton, Gregory Frederick
Electric Power Research Institute

September 2024

Prepared by

OAK RIDGE NATIONAL LABORATORY
Oak Ridge, TN 37831-6283
managed by
UT-BATTELLE, LLC
for the
US DEPARTMENT OF ENERGY
Office of Nuclear Energy

under contract DE-AC05-00OR22725

CONTENTS

LIST OF FIGURES

LIST OF TABLES

ACRONYMS

ABSI-LW	auxiliary beam stress improved laser welding
appm	atom parts per million
DIC	digital image correlation
DOE	Department of Energy
EDM	electrical discharge machining
EPRI	Electric Power Research Institute
FSW	friction stir welding
HAZ	heat-affected zone
HeIC	helium induced cracking
LTO	Long-Term Operation
LW	laser weld
LWRS	Light Water Reactor Sustainability
NE	Office of Nuclear Energy
ORNL	Oak Ridge National Laboratory
SEM/EDS	scanning electron microscopy/energy-dispersive X-ray spectroscopy
THDS	thermal helium desorption spectroscopy
VAR	vacuum arc melting
VTI	Vacuum Technology Incorporated
wppm	weight parts per million

ACKNOWLEDGMENT

This research was sponsored by the US Department of Energy (DOE), Office of Nuclear Energy (NE), under contract No. DE-AC05-00OR22725 with Oak Ridge National Laboratory (ORNL), managed and operated by UT-Battelle, LLC. Programmatic support was provided by DOE Office of Nuclear Energy (DOE-NE), Light Water Reactor Sustainability Program Materials Research Pathway.

The authors gratefully acknowledge the program support of Xiang (Frank) Chen, Materials Research Pathway Lead of the Light Water Reactor Sustainability Program at ORNL; engineering support of Kurt Smith and Bob Sitterson; hot cell facilities and operations contributions of Clay Morris, Jerid Metcalf, Tony Davis, Kevin Delabar, Rick Bowman, Scott Thurman, Scott White, Donald Caverly, and Allen Smith.

ABSTRACT

This report summarizes the most recent welding campaign on irradiated Ni-base alloy 182 and the preliminary weld quality inspections at the Radiochemical Engineering Development Center (REDC). Equipment and capabilities were developed jointly by the U.S. Department of Energy, Office of Nuclear Energy, Light Water Reactor Sustainability Program, the Electric Power Research Institute, Long Term Operations Program (and the Welding and Repair Technology Center), and Oak Ridge National Laboratory. Irradiated nickel alloy 182 with doped boron up to 23wppm were laser welded in the hot cell successfully based on initial in-cell camera examination. The significant, on-going effort to weld irradiated alloys with high helium concentrations and comprehensively analyze the results will eventually yield validated repair techniques and guidelines for use by the nuclear industry in extending the operational lifetimes of nuclear power plants.

This report fulfills the FY 2024 milestone M2LW-24OR0406013, "Complete the second weld campaign on Ni alloy 182 using optimized welding parameters and complete the initial weld quality evaluation".

1. INTRODUCTION

Today, welding is widely used for repair, maintenance, and upgrades of nuclear reactor components. As a critical technology to extend the service life of nuclear power plants beyond 60 years, weld technology must be further developed to meet new challenges associated with the aging of the plants, such as control and mitigation of the detrimental effects of weld residual stresses and repair of highly irradiated materials. To meet this goal, a fundamental understanding of welding effects is necessary for the development of new and improved welding technologies.

Welding repair of irradiated nuclear reactor materials (such as austenitic stainless steels used for the reactor internals) is very challenging because the existence of helium in the steel, even at very low levels (*i.e.*, parts per million), can cause cracking during repair welding. Helium is a product of the boron and nickel transmutation process under intense neutron irradiation. Under the influence of high temperatures and high tensile stresses during welding, rapid formation and growth of helium bubbles can occur at grain boundaries, resulting in intergranular cracking in the heat-affected zone (HAZ) – the so-called helium-induced cracking (HeIC) (Kanne Jr. 1988). Over the past decades, a basic understanding has been established for the detrimental effects of weld stresses on HeIC (Feng and Wilkowski 2002) (Feng, Wolfe, *et al*. 2009). However, practical methods for weld repair of irradiated materials are still evolving. Industry's experience is based on current arc-welding–based and laser-welding–based repair technologies that are limited to situations where the helium in the irradiated materials is less than 10 appm. Although no welding restrictions are required for helium levels below 0.1 appm helium, restrictions on welding parameters, such as welding heat input, are necessary when the helium levels are above 0.1appm. Reactor internals with helium levels above 5-10 appm are generally considered not to be weldable (or weld repairable) using today's welding practices common to the industry (EPRI 2015) (JNES 2004).

As the service life of nuclear reactors in the United States is extended, the amount of helium in the structural materials in certain highly irradiated areas will continue to increase, reaching levels much higher than 10 appm. Therefore, innovations in repair welding technology are essential to addressing this critical industry need.

This research, a joint effort of the US Department of Energy Office of Nuclear Energy (DOE-NE) Light Water Reactor Sustainability (LWRS) Program and the Electric Power Research Institute (EPRI) Long-Term Operations (LTO) Program and Welding and Repair Technology Center, is aimed at developing advanced welding technology for reactor repair and upgrades. It focuses on welding repair of irradiated materials that are extremely challenging and require long-term R&D. Multiple weld campaigns have been completed on irradiated 304 and 316 stainless steels with the targeted helium concentration up to 30 appm between FY2018 and FY2021. Microstructural characterizations demonstrated the feasibility to use advanced auxiliary beam stress improved laser welding (ABSI-LW) to mitigate the formation of HeIC. In FY2022 and FY2023, irradiated nickel alloy 182 samples were further studied using ABSI-LW (M3LW-22OR0406013). The microstructural characterization showed no major cracks in most of the HAZ in welded samples with dopped boron concentration up to 15 wppm, except for weld toe regions as shown in **Figure 1**. Hence, the research activities in FY2024 focused on further optimization of the laser welding parameters to mitigate this issue (M3LW-23OR0406015). This milestone report summarizes the progress of the research activities and the second weld campaign conducted on irradiated Ni-base irradiated materials at the Radiochemical Engineering Development Center (REDC).

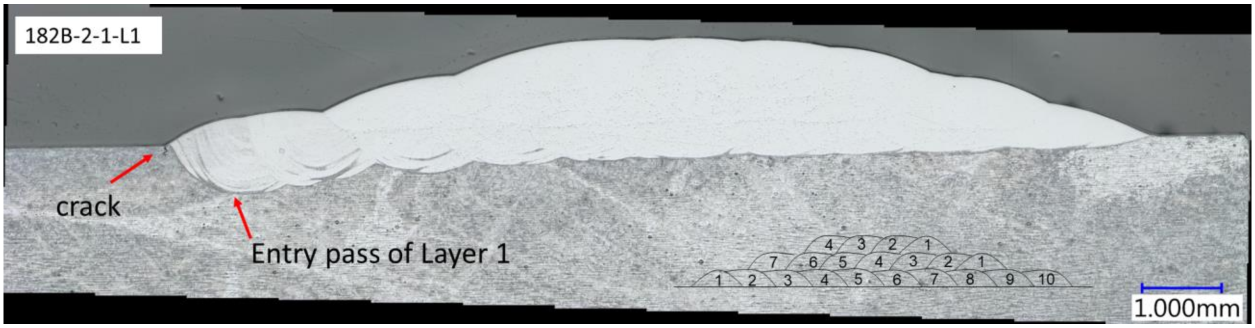

Figure 1 A weld cross-section produced in the previous weld campaign (M3LW-22OR0406013) showing a small crack in the toe region of the entry pass.

2. EXPERIMENTS

2.1 Materials

Five heats of Alloy 182 having five boron concentration levels (nominally 0, 5, 10, 20, and 30 ppm by weight) were produced by Sophisticated Alloys, Inc, following the specifications established by ORNL to cover the anticipated range of helium levels in materials exposed up to 80 years of reactor operation (M3LW-14OR0406014, 2014). Table **1** shows the complete chemistry analysis of the Alloys 182 heats used in this project. As shown in the Table 1 not all the target boron concentrations were achieved but a wide range of boron levels were produced ranging from 0.3 to 23 wppm. All other elements met the chemistry requirements for Alloy 182. Bar stock sections were machined to final dimensions ($76x56x8.9mm^3$ nominal) to yield 7 pieces at each boron level for subsequent irradiation. Alloy 182, being weld filler metal, typically has a coarser weld microstructure in reactor structures. An additional fifteen specimens from heats 182D and 182E respectively were fusion welded on one side to half of the specimen depth to produce a representative weld microstructure.

The custom alloy 182 blocks were irradiated at the ORNL High Flux Isotope Reactor with a total fluence ranging from 5.08×10^{20} to 1.31×10^{21} depending on the location of the blocks inside the irradiation bores. The irradiated blocks were aged for more than 2 years to allow decay of short half-life isotopes before welding experiments began. Details of the irradiation of the coupons can be found in the previous milestone report M3LW-17OR0406013 (Feng, Miller, *et al*. 2017).

Table 1 Chemistry Analysis Results of Alloy 182

Element	Unit	Alloy 182 Heat Identification				
		182A	182B	182C	182D	182E
B	wppm	0.3	5	15	14	23
Co	wppm	2	2	2	2	2
Al	wppm	81	34	32	54	56
Mo	wppm	1	1	8	1	1
Cu	wppm	2	1	2	1	1
C	wt%	0.03	0.08	0.03	0.04	0.04
Mn	wt%	7.03	7.00	6.76	7.17	7.08
Si	wt%	0.50	0.50	0.51	0.50	0.49
Cr	wt%	15.99	16.00	16.00	16.16	16.10
Fe	wt%	7.36	7.92	7.31	7.14	7.12
Nb	wt%	2.07	2.06	1.83	1.82	1.84
Ti	wt%	0.44	0.43	0.43	0.43	0.46
P	wt%	0.00013	0.00011	0.00018	0.00015	0.00016
S	wt%	0.00207	0.00199	0.00280	0.00200	0.00220
Ni		Balance	Balance	Balance	Balance	Balance

2.2 Welding

In this weld campaign, laser welding experiments were conducted on three alloy 182 coupons with three nominal boron concentrations (10, 20 and 30 wppm). The weld coupon ID, measured boron concentrations, welding process, and weld campaign identification are given in **Table 2.** Details of the equipment and experimental procedures have been reported in the previous milestone report (M2LW-17OR0406014) (Feng, Miller, *et al*. 2017).

Table 2 Weld Coupon ID

Weld Coupon ID.	Microstructural condition	Target Boron, wppm	Measured boron, wppm
182C-4	Wrought	10	15
182D-3	Wrought	20	14
182E-1	Wrought	30	23

Figure 2 shows the laser welding equipment consisting of two IPG lasers. One is for welding (1.5kW) and the other (2.0 kW, defocused) is connected to a Galvo-scanners providing auxiliary heating patterns to improve the stress distribution around weld pool.

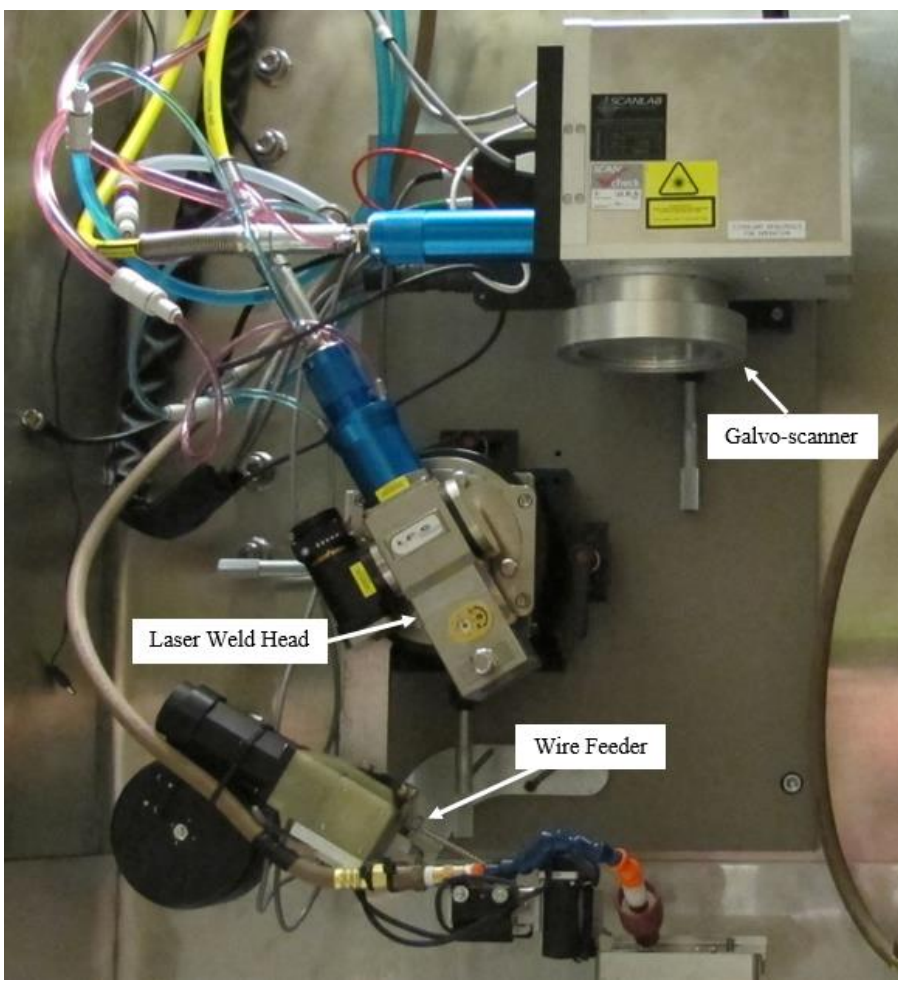

Figure 2 Dual-beam laser welding equipment.

Laser weld cladding was performed on irradiated alloy 182 base material with 82 as filler material. Four laser-welded clads (weld IDs L1, L2, L3 and L4) were made using different welding conditions on each coupon. The arrangement of the four laser clads on each coupon was similar to the previous weld campaign (M3LW-22OR0406013) as illustrated in Figure 3. In this figure, the two three-layer claddings on the top side of the steel coupon plate are labeled as L1 and L2, and two claddings on the bottom side are labeled as L3 and L4. Weld claddings L2 and L4 in the figure were made with the ABSI-LW and weld claddings L1 and L3 were made with LW without ABSI for comparison. Each clad consisted of three layers (Layer 1, layer 2 and Layer 3 from the bottom to the top of each clad). Layer 1 consisted of ten weld passes. Layer 2 consisted of seven weld passes. Layer 3 consisted of four weld passes. The welding sequence of each layer is denoted using the numerical numbers as shown in **Figure 3.**

There are two major differences in terms of the laser parameters from the previous weld campaign:

(a) The power of the welding beam was reduced from 1000W to 700W for the entry pass of each layer (Pass 1 of Layer 1, Pass 1 of Layer 2, and Pass 1 of Layer 3).

(b) After welding each 3-layer clad, one additional autogenous pass (no filler wire) on each side of the weld toe regions of the first layer was performed as highlighted in red color in **Figure 3**. The center of the autogenous pass was aligned with the edge of the weld toe where the crack occurred in the last weld campaign (refer to **Figure 1**)

The purpose of these adjustments is to reduce and mitigate the formation of crack in the weld toe regions as observed in the previous weld campaign.

Single-pass weld without auxiliary beam (labeled as SL or SH) was also conducted. The purpose is to validate the effective heat input after the weld samples are cut. Since SL and SH with 1000W beam power has been studied in the previous campaign, the laser power of SL and SH used in this current campaign was reduced to 700W, identical to the power of the entry pass of the first layer of each clad. The relative locations of the single-pass welds are indicated in **Figure 3**. The welding direction of all weld passes was consistently towards the positive direction of the X axis. The Y-coordinates of the first and the last weld passes in Layer 1, as well as the Y- coordinates of the single pass welds, were also shown in **Figure** 3.

182C-4

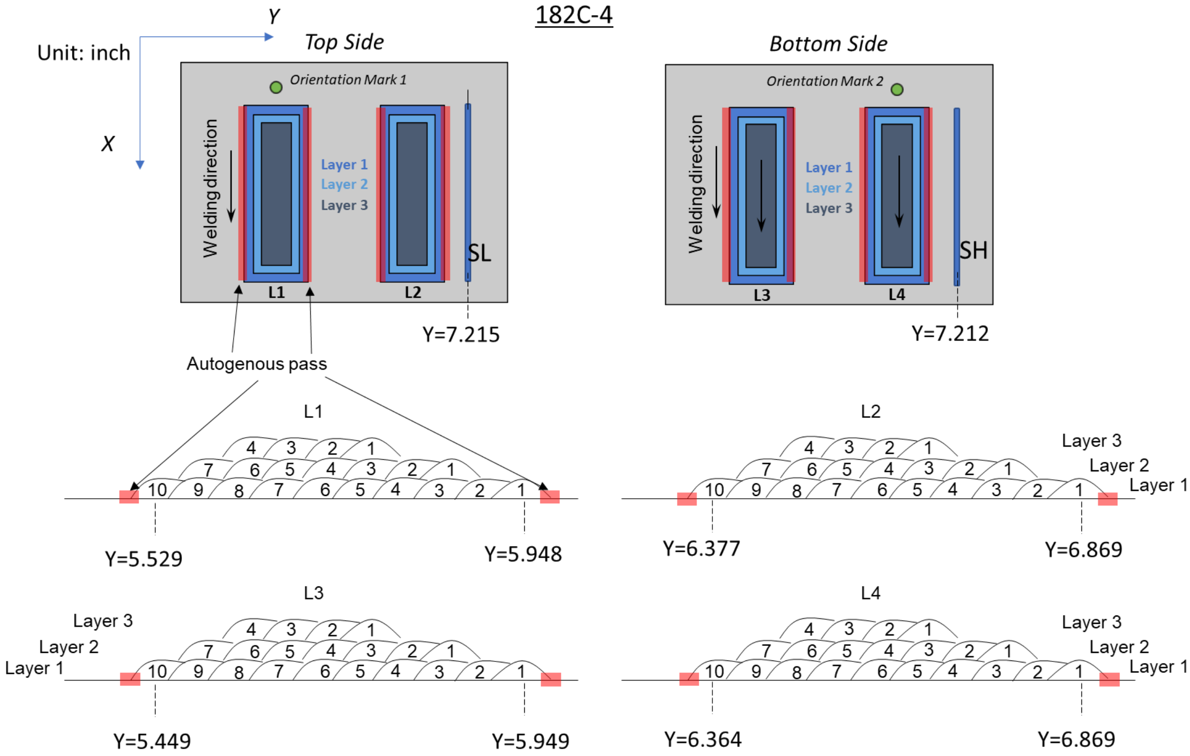
Unit: inch
Y
X
Top Side
Orientation Mark 1
Welding direction
Layer 1
Layer 2
Layer 3
SL
L1
L2
Y=7.215
Autogenous pass
Bottom Side
Orientation Mark 2
Welding direction
Layer 1
Layer 2
Layer 3
SH
L3
L4
Y=7.212
L1
Y=5.529
Y=5.948
L2
Layer 3
Layer 2
Layer 1
Y=6.377
Y=6.869
L3
Layer 3
Layer 2
Layer 1
Y=5.449
Y=5.949
L4
Layer 3
Layer 2
Layer 1
Y=6.364
Y=6.869

182D-3

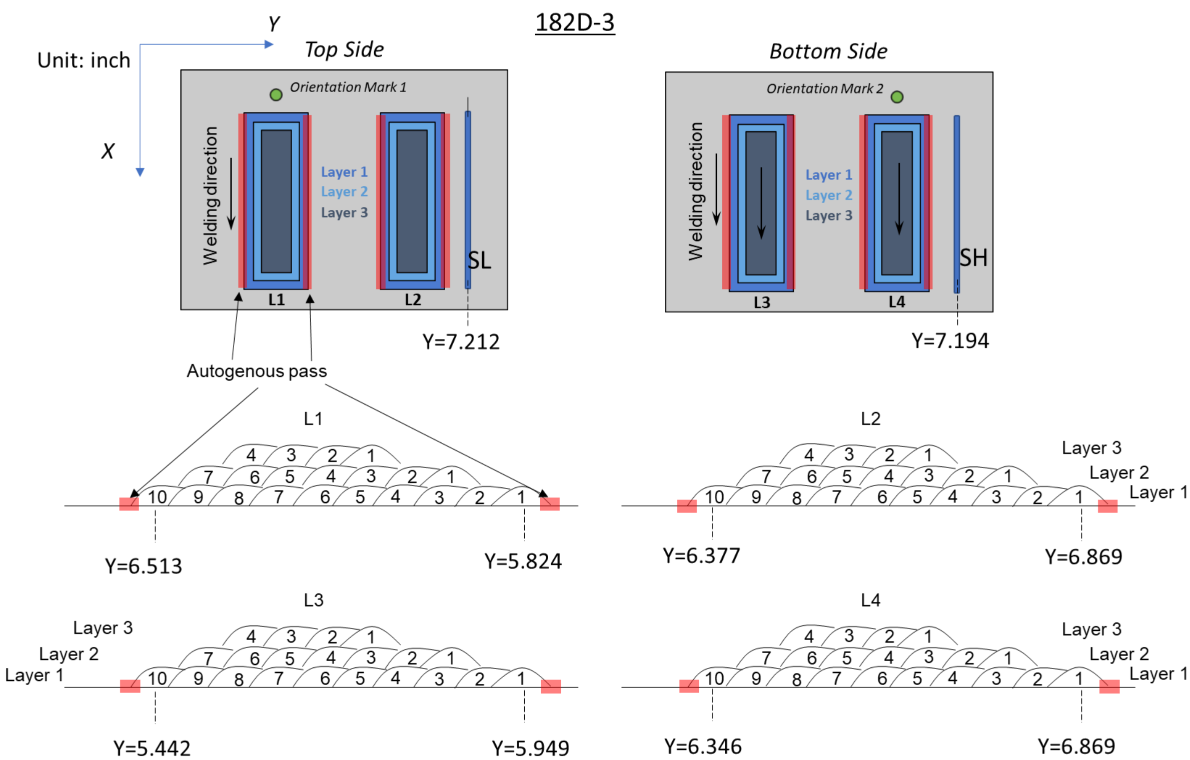
Unit: inch
Y
X
Top Side
Orientation Mark 1
Welding direction
Layer 1
Layer 2
Layer 3
SL
L1
L2
Y=7.212
Autogenous pass
Bottom Side
Orientation Mark 2
Welding direction
Layer 1
Layer 2
Layer 3
SH
L3
L4
Y=7.194
L1
Y=6.513
Y=5.824
L2
Layer 3
Layer 2
Layer 1
Y=6.377
Y=6.869
L3
Layer 3
Layer 2
Layer 1
Y=5.442
Y=5.949
L4
Layer 3
Layer 2
Layer 1
Y=6.346
Y=6.869

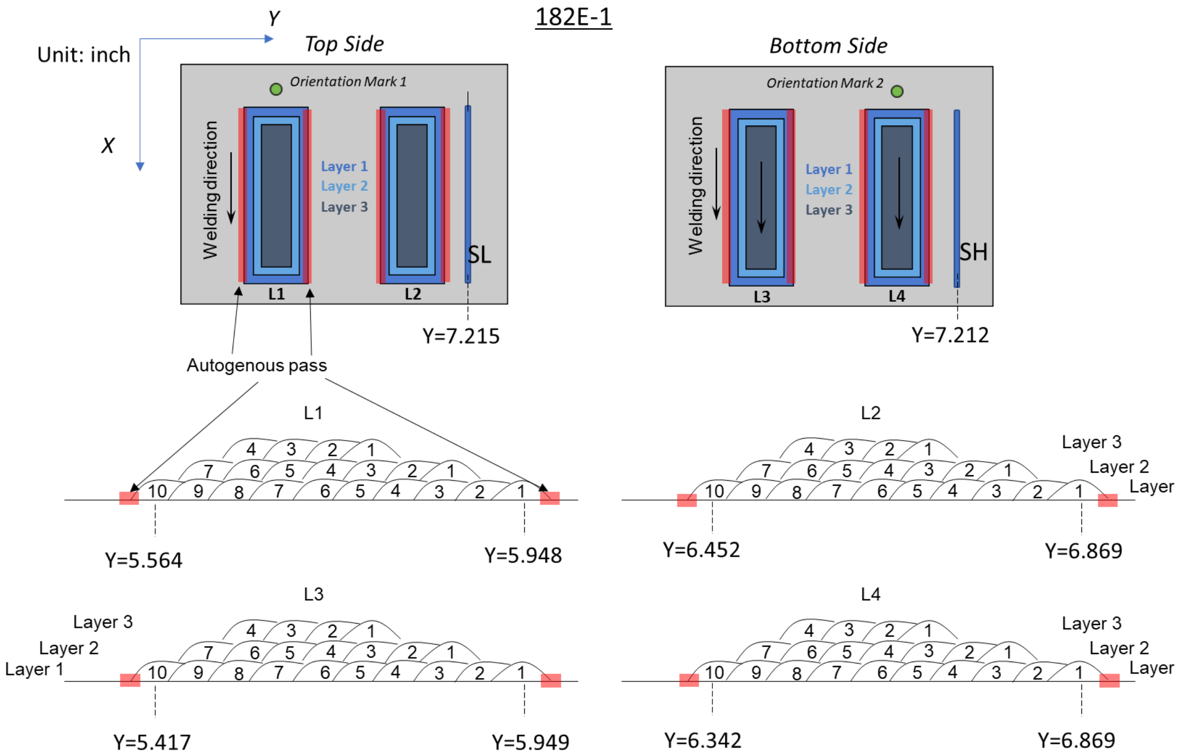

Figure 3 Weld Layout for LW of Irradiated Coupons.

The essential laser weld cladding parameters are given in **Table 3.** Typically, within each completed cladding, identical welding parameters were applied. Weld clads L1 and L2 had a higher laser cladding speed and low heat input than weld clads L3 and L4 in these experiments. Therefore, each weld coupon had four weld claddings (L1 through L4) performed with four different welding conditions. Additional single-pass LW passes without ABSI, labeled as SL and SH in **Figure 3,** were performed to evaluate the effect of heat input and weld bead profile of a single LW pass on HeIC. The letter "S" in the label stands for single-pass weld. "L" or "H" stands for low-heat or high-heat parameter set. This provides the ability to isolate the effect of multi-thermal cycles in the multi-pass, multi-layer clads. Single pass welds also allow for the determination of the base metal percentage dilution of the first weld layer by for each LW parameter set. The percentage Base Metal Dilution = 100 X (Area of Base Metal Melted /Area of Deposited Weld). Furthermore, the weld dilution may also be used to estimate what the maximum helium content of the first layer or individual weld pass could be assuming the helium does not escape the weld pool. It is expected that only a portion of the helium remains in the first weld layer or individual weld pass and successively lower amounts as more layers are applied. Removing specimens for helium measurement to determine the percentage helium remaining also provides an estimate of how many layers are required before conventional welding methods may be used to complete the reactor repair or modification. The welding condition for SL was identical to the parameters of the entry pass in L1; The welding condition for SH was identical to the parameters of the entry pass in L3. The basic laser welding parameters are summarized in **Table 3.** The different welding speeds and corresponding wire feed rates resulted in different individual weld and clad layer thicknesses.

Note, abnormal welding parameters or conditions were accidentally used in some of the passes. They are summarized as follows:

(a) Sample ID 182C-4: insufficient shielding gas in weld passes 1 and 2 in Layer 1of clad L2.

(b) Sample ID 182D-3: insufficient shielding gas in weld pass 5 in Layer 1of clad L4.

(c) Sample ID 182E-1: insufficient shielding gas from Pass 5/ Layer 2 to Pass1/layer 2 in clad L4.

Table 3 Laser Weld Cladding Parameters

Parameter	Multi-pass Weld Clads				Single-Pass Weld	
	L1	**L2**	**L3**	**L4**	**SL**	**SH**
Travel speed (in./s)	0.45 (high-speed)	0.45 (high-speed)	0.083 (low-speed)	0.083 (low-speed)	0.45 (high-speed)	0.45 (high-speed)
Expected effective heat input from welding beam (kJ/in)	0.39 (low-heat)	0.39 (low-heat)	1.20 (high-heat)	1.20 (high-heat)	0.39 (low-heat)	1.20 (high-heat)
Wire feed speed (in./min)	50	50	13.1	13.1	50	13.1
Welding laser power for the entry pass of each layer (W)	***700***	***700***	***700***	***700***	***700***	***700***
Welding laser power for the rest of passes (W)	1,000	1,000	1,000	1,000	N/A	N/A
Welding laser power for autogenous pass on both sides of each clad (W)	***430***	***430***	***660***	***660***	N/A	N/A
Welding laser diameter (mm)	2	2	2	2	2	2
ABSI	No	Yes	No	Yes	No	No
ABSI laser power (W)	N/A	2000	N/A	368	N/A	N/A
ABSI laser diameter (mm)	N/A	7.5	N/A	7.5	N/A	N/A

2.3 Weld quality inspections

The preliminary weld quality inspection was conducted right after each clad was completed using the inline camera in the laser system. More detailed cross-sectional microstructural characterization is in progress and will be reported in the next fiscal year.

3. RESULTS AND DISCUSSION

Figure 4 shows the surface weld quality of twelve weld clads after completion of each clad using the in-line camera on the laser system. No macroscopic cracking (i.e, greater than millimeter size) or other defects were observed under visual inspection.

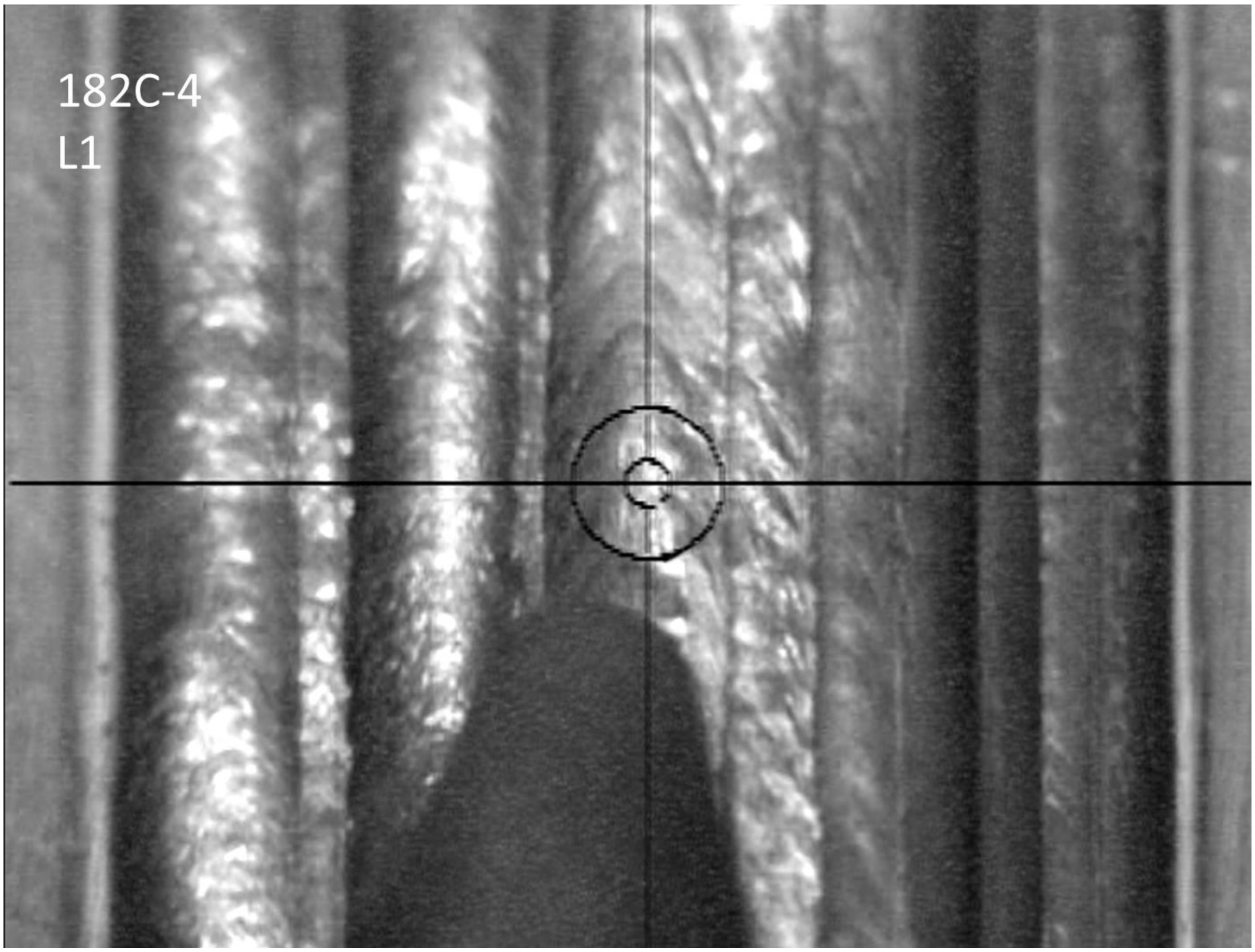

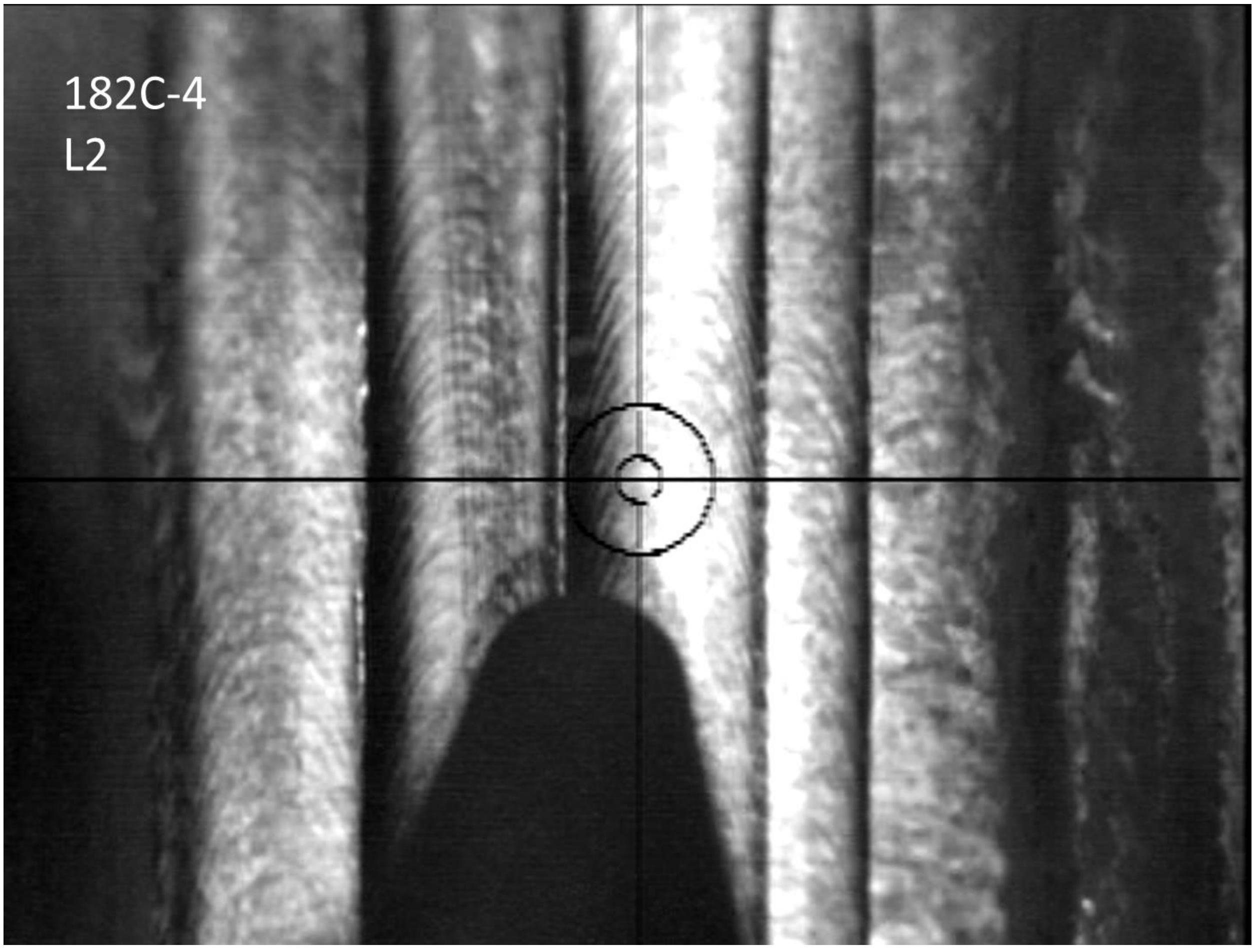
182C-4
L2

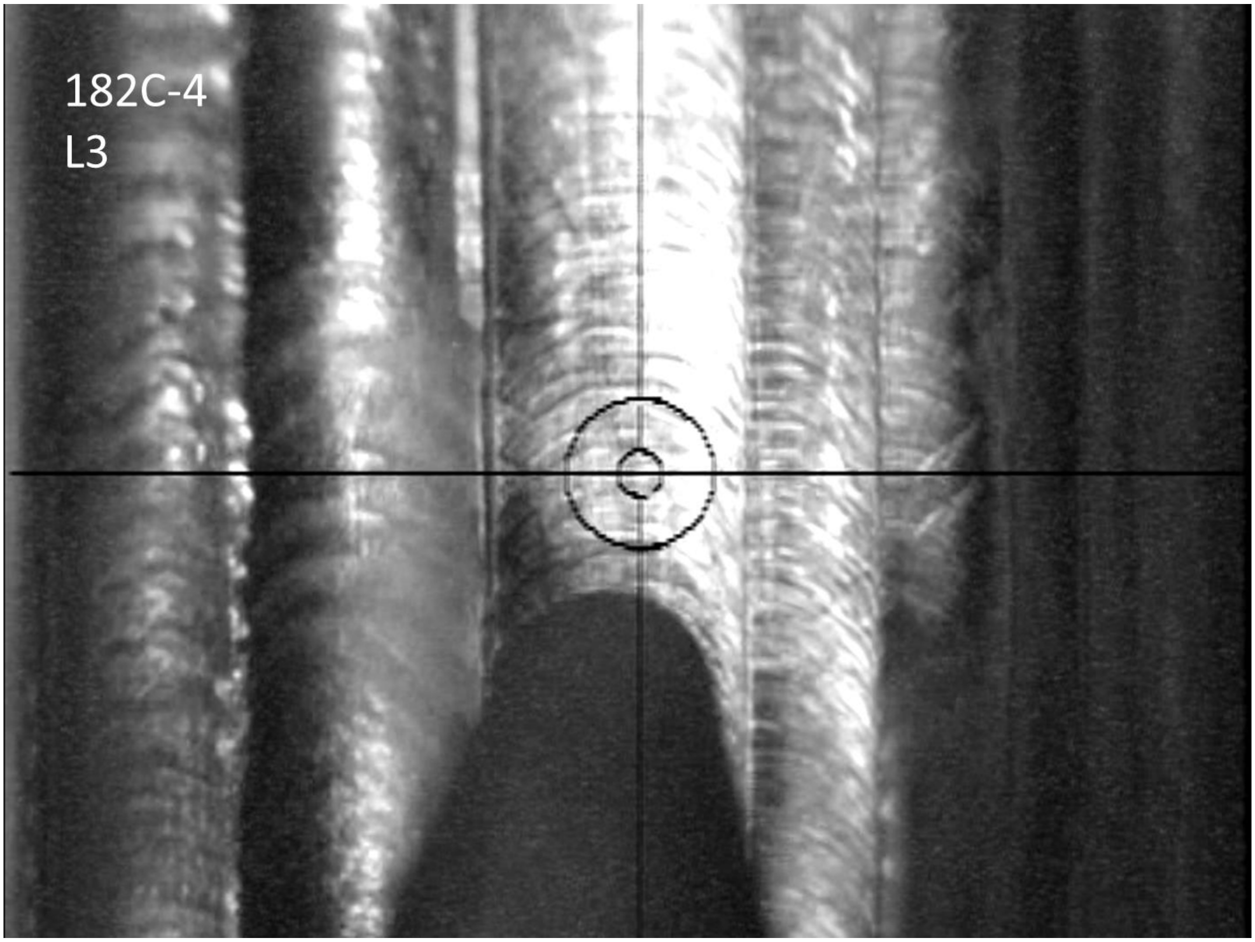
182C-4
L3

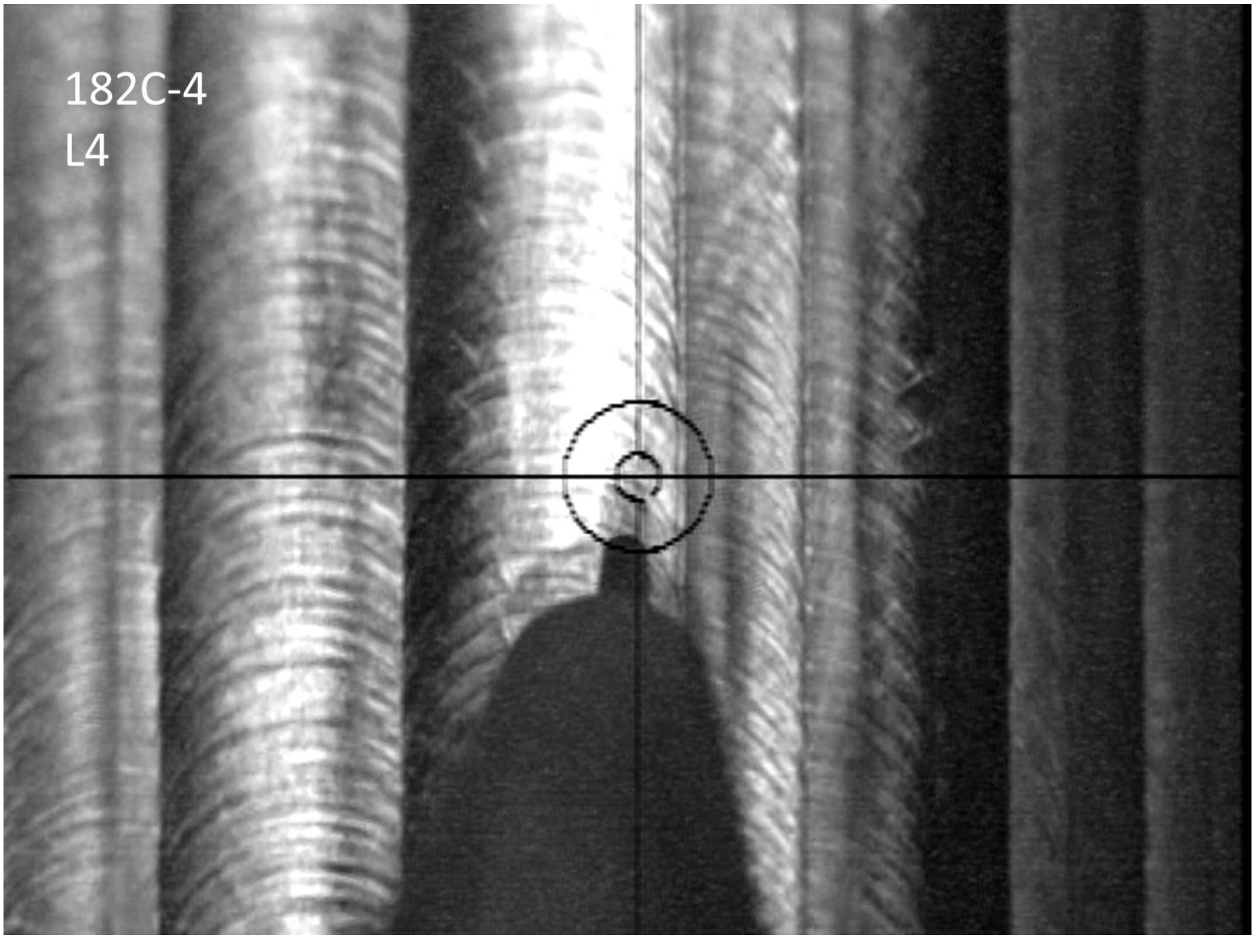
182C-4
L4

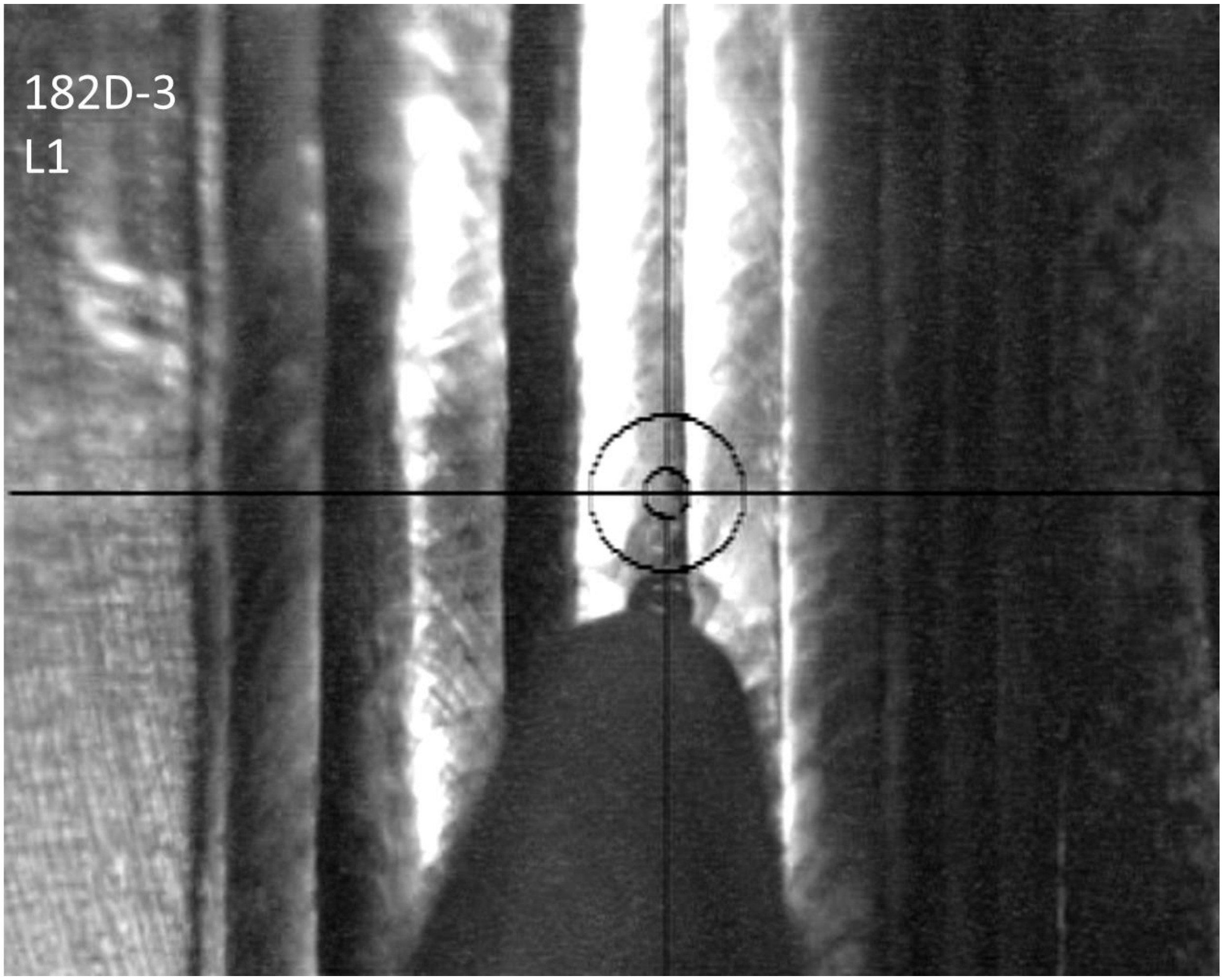
182D-3
L1

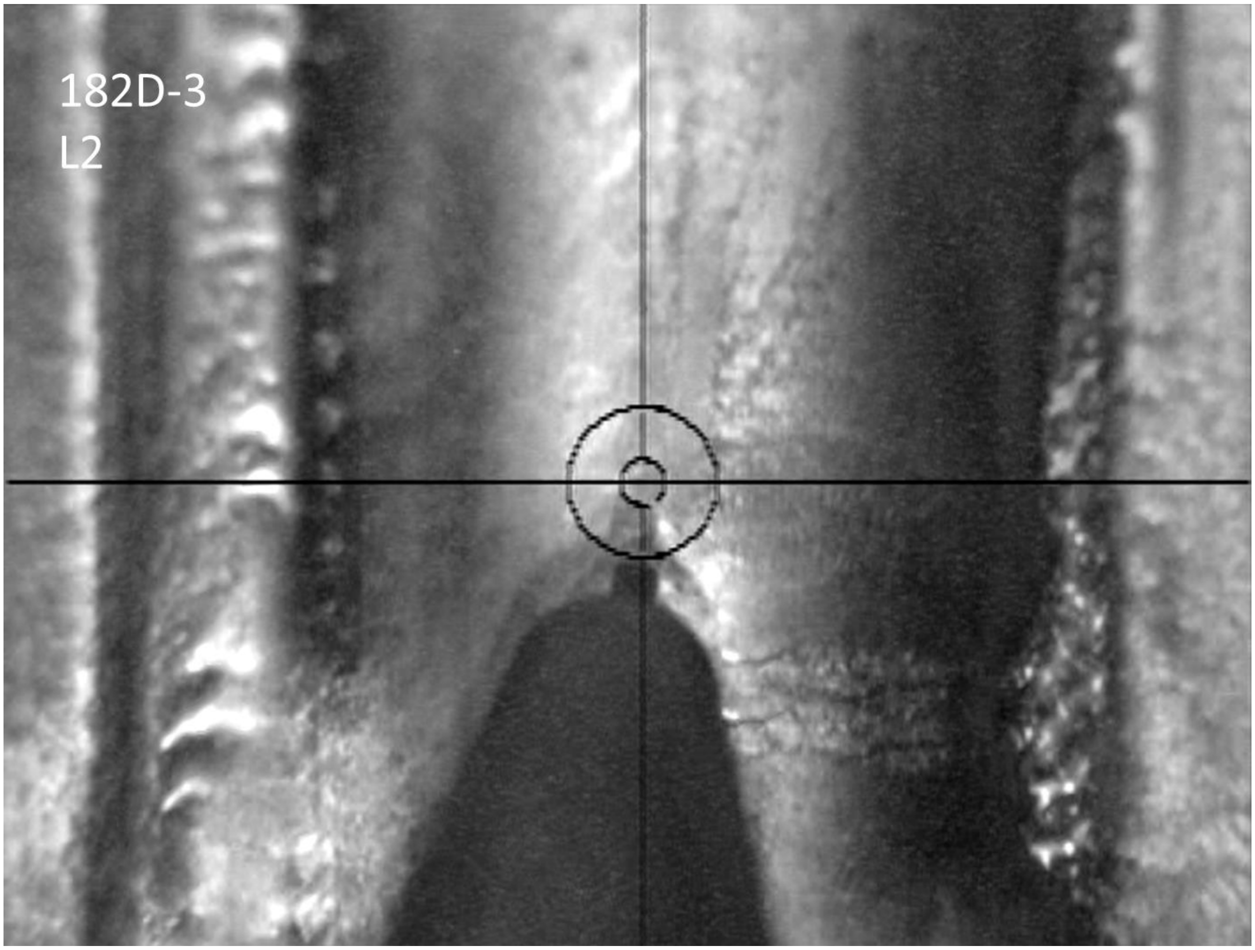
182D-3
L2

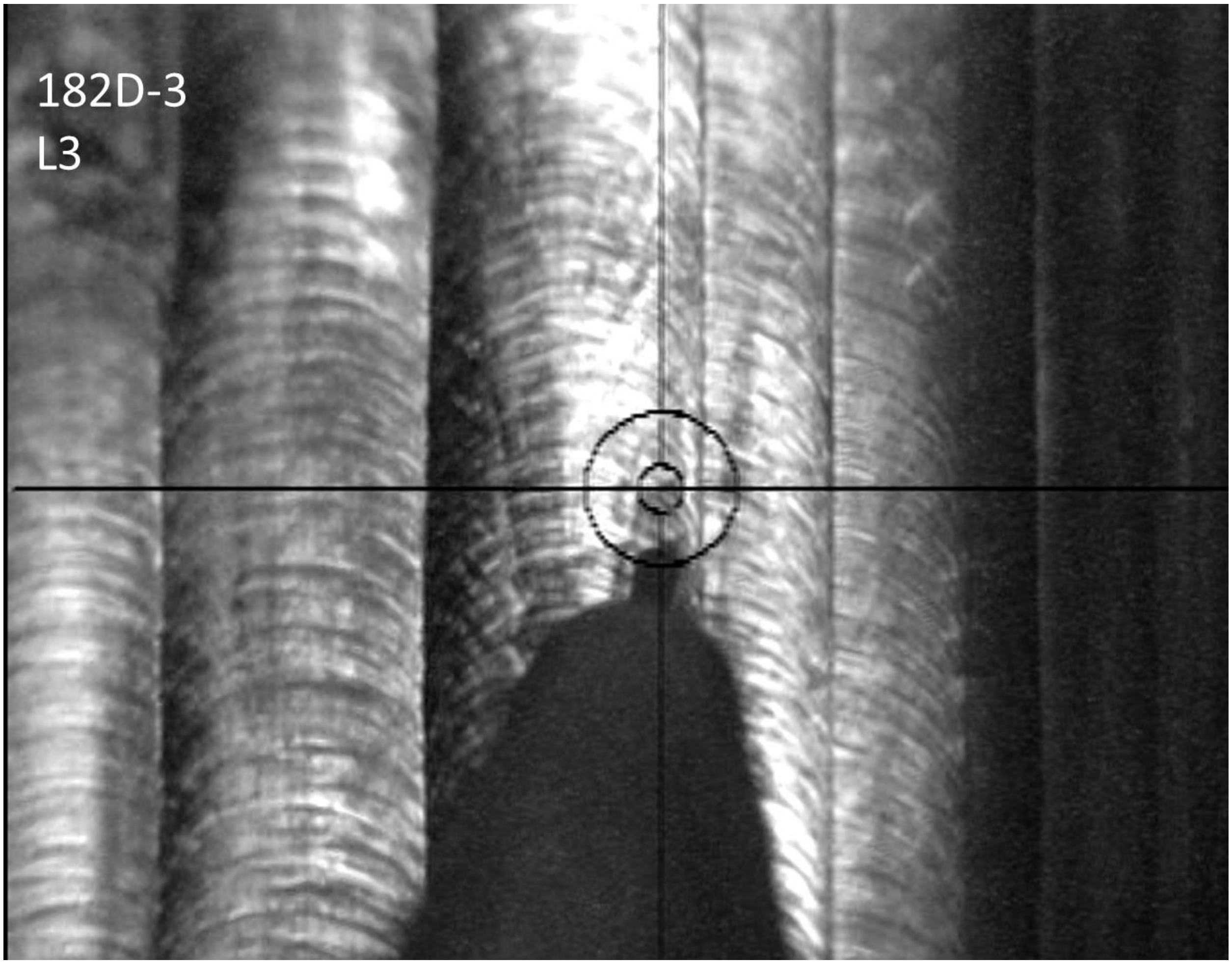
182D-3
L3

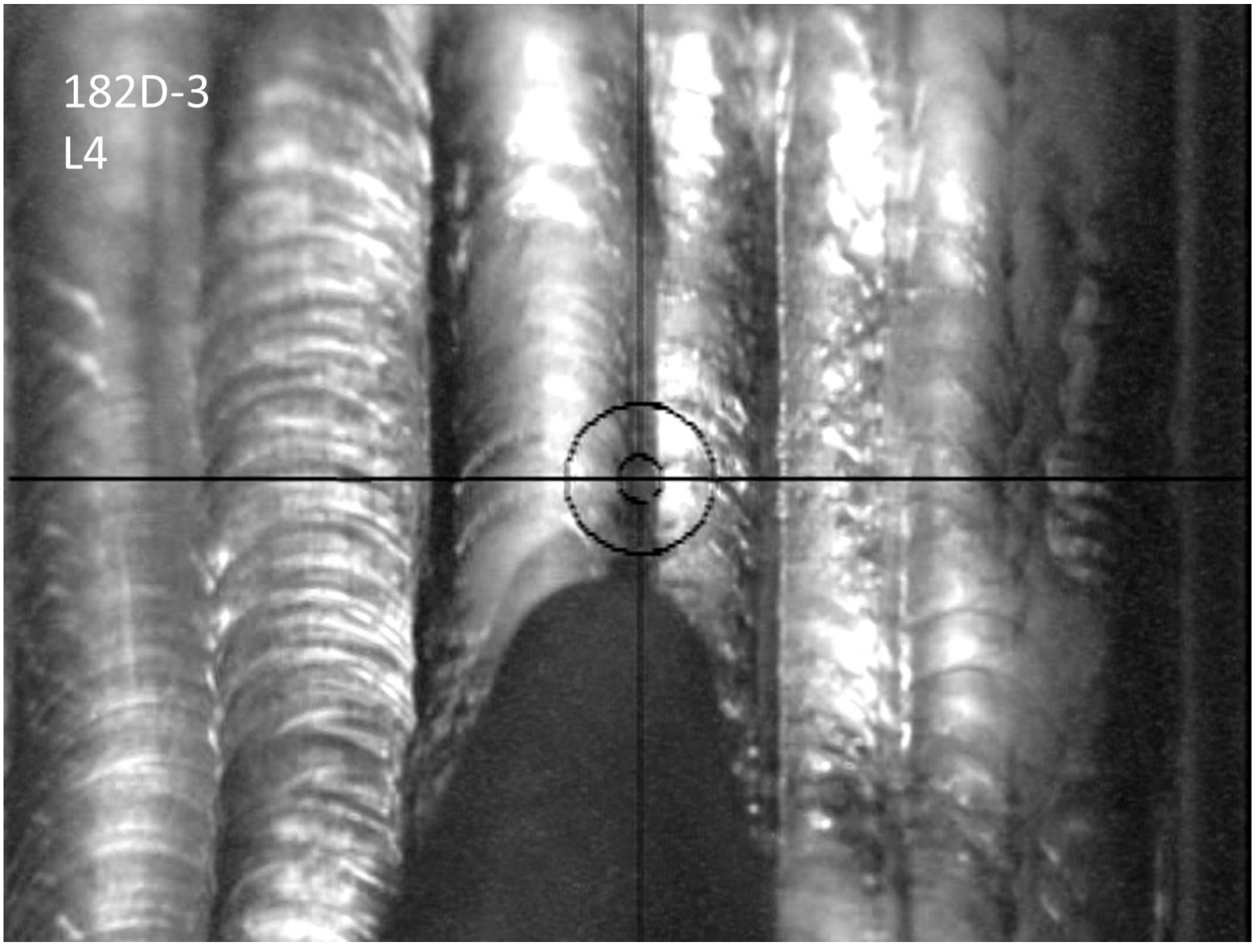
182D-3
L4

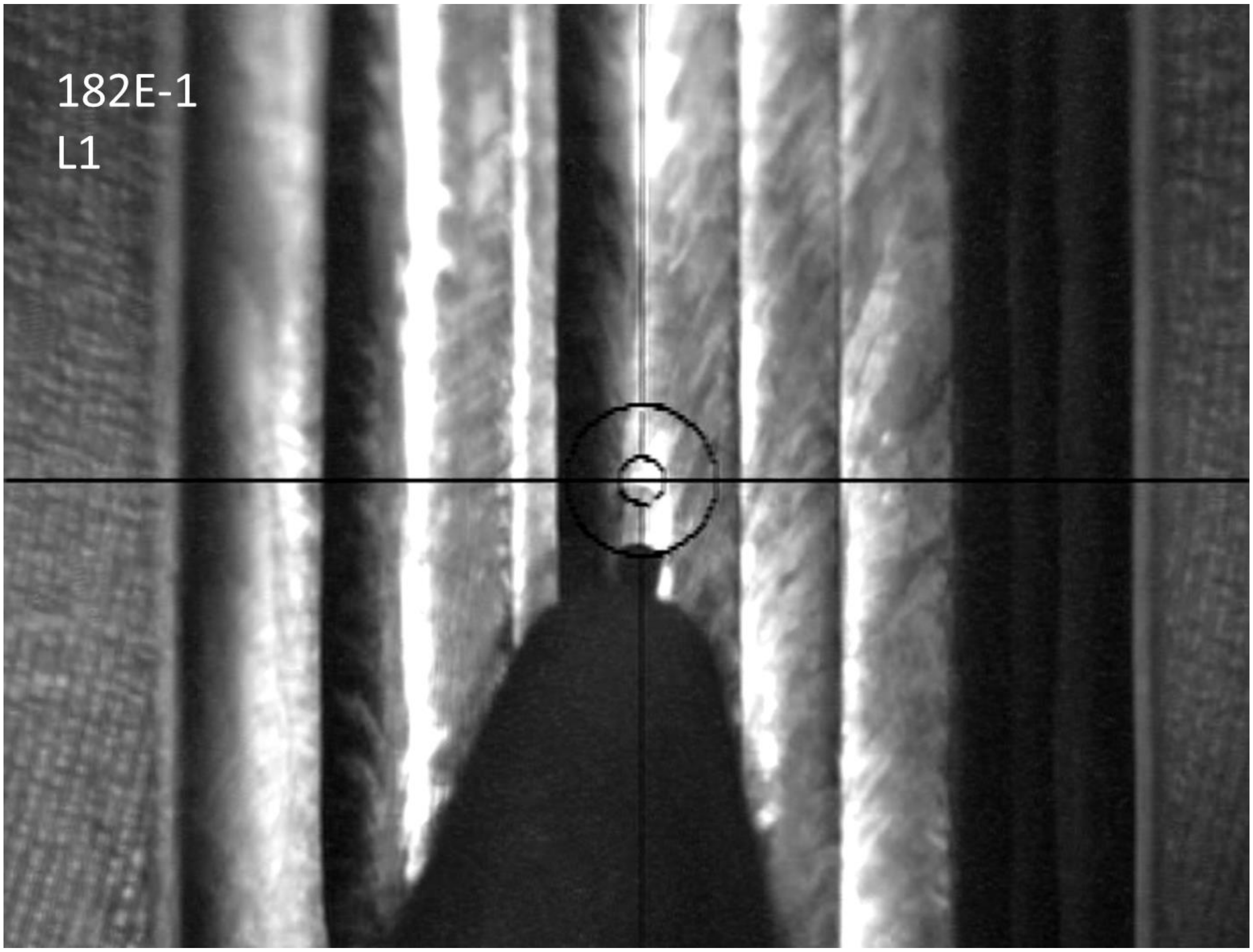
182E-1
L1

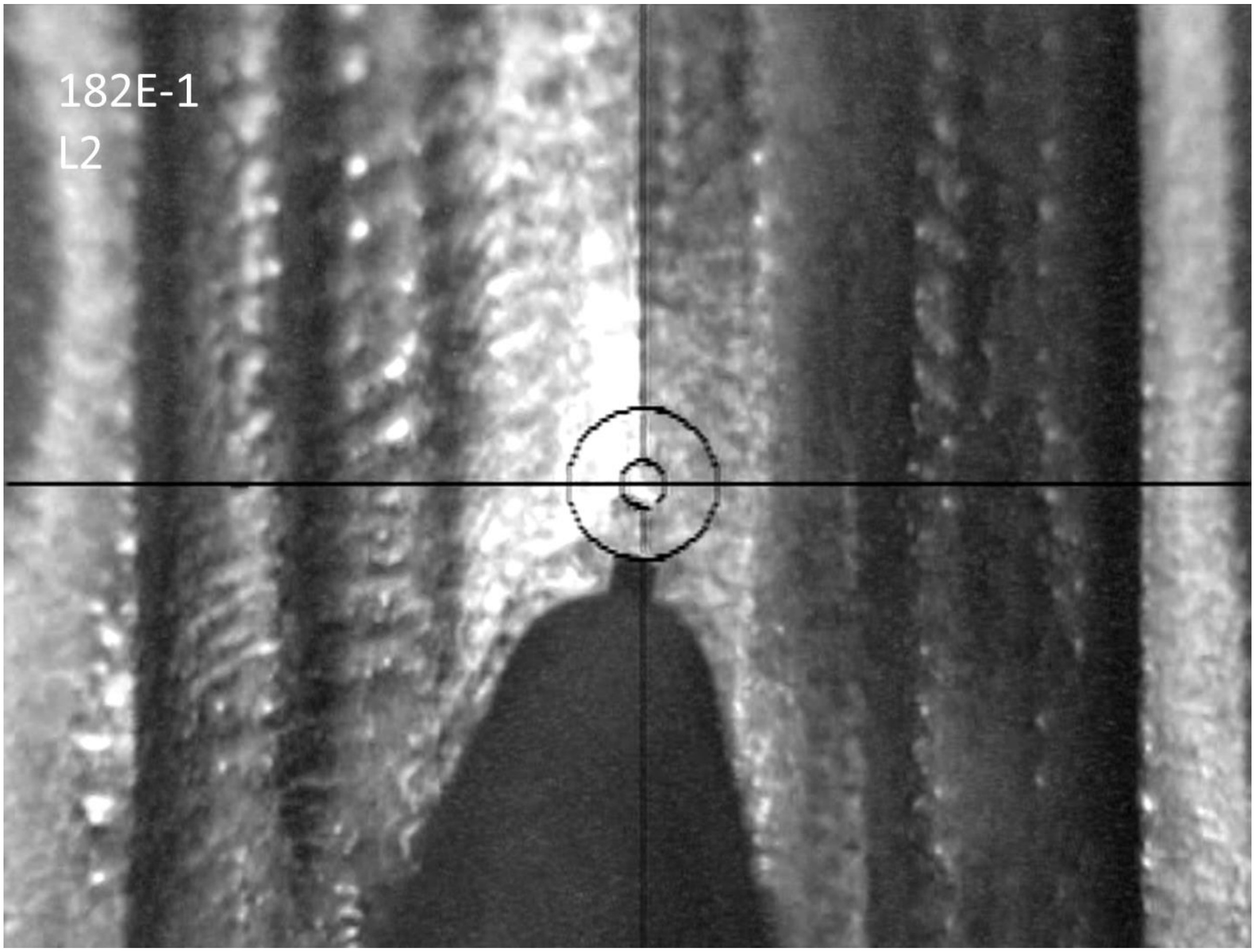
182E-1
L2

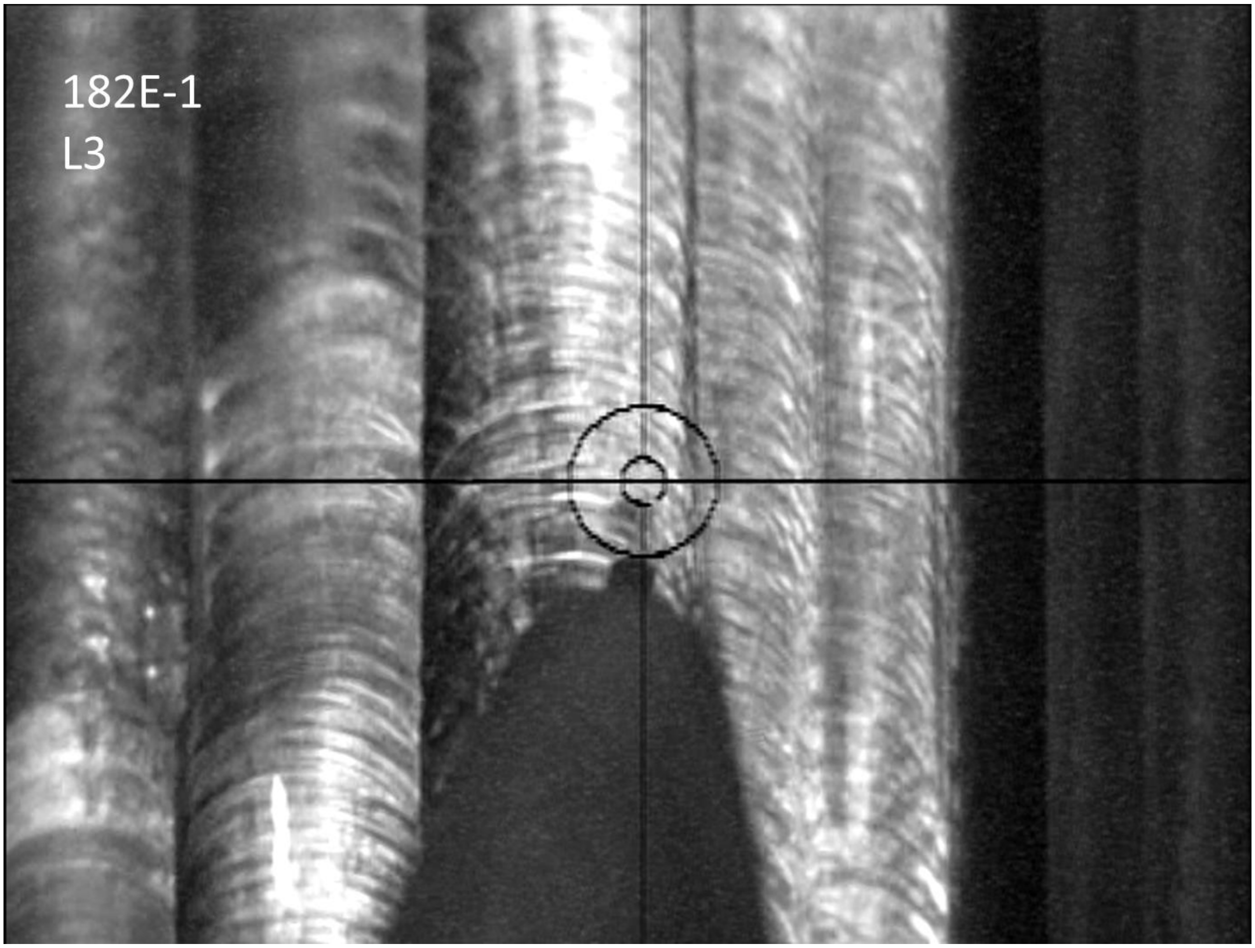
182E-1
L3

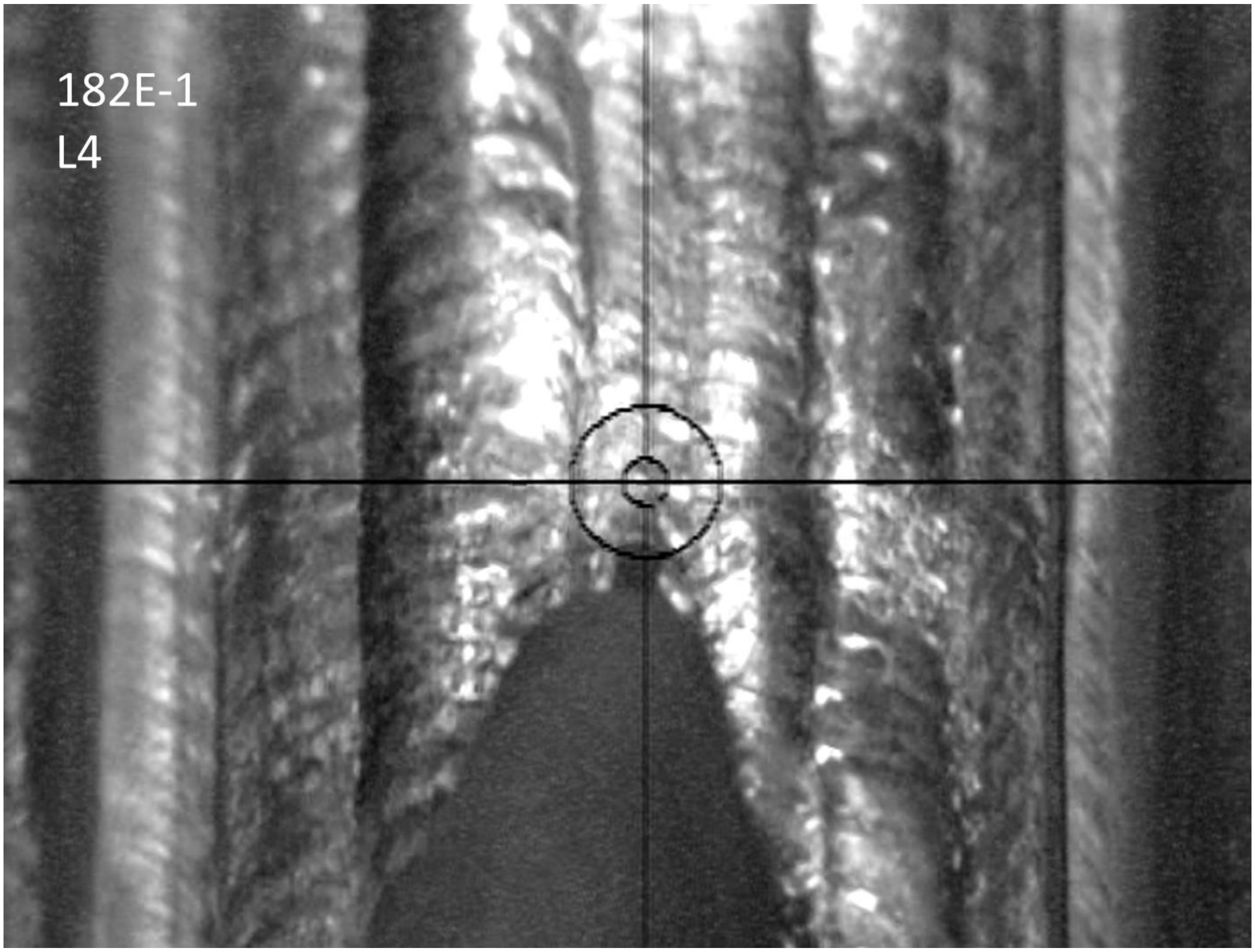

Figure 4 Initial surface inspection of the welded Alloy 182 coupons.

After welding each 3-layer clad, one additional autogenous pass (no filler wire) on each side of the weld toe regions of the first layer was performed. **Figure 5** shows the examples of 430W and 660W autogenous welding of the entry-pass side in clads L1 (low heat input without ABSI) and L3 (high heat without ABSI) respectively in Coupon 182E-1.

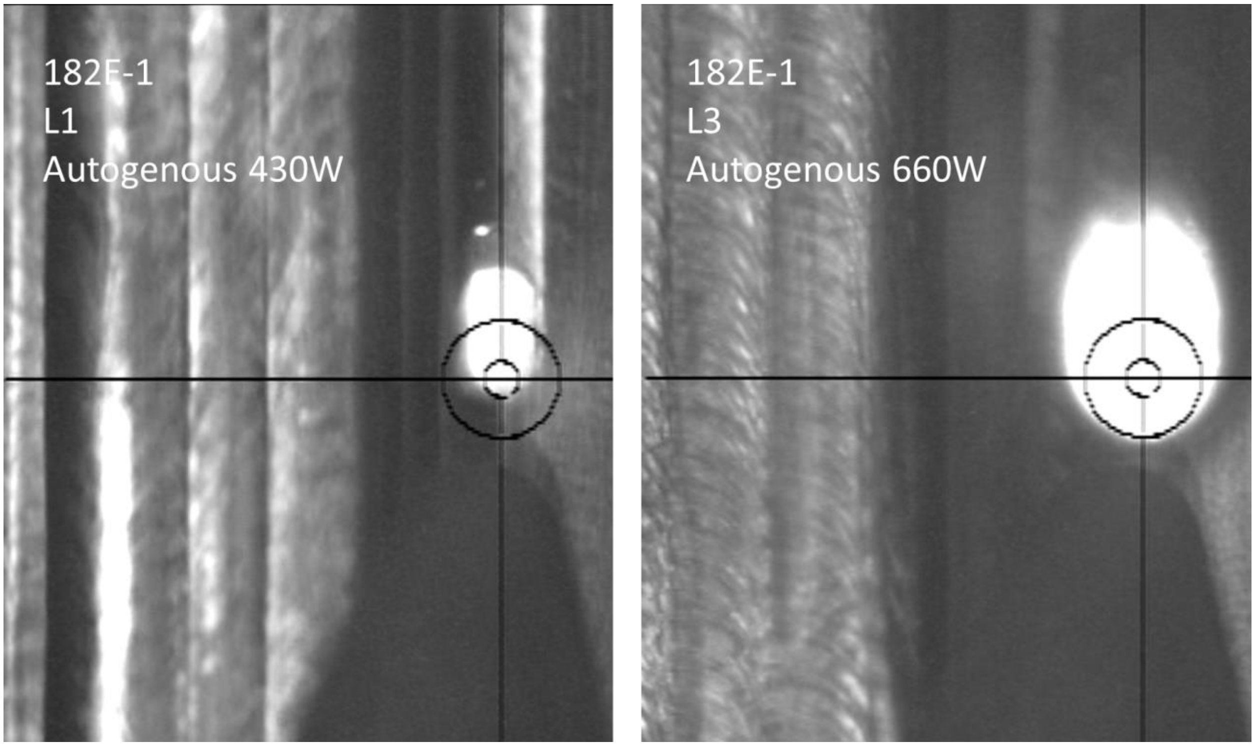

Figure 5 Examples of 430W and 660W autogenous welding of the entry-pass side in clads L1 (low heat input without ABSI) and L3 (high heat without ABSI) respectively in Coupon 182E-1.

4. SUMMARY

This report summarizes the second campaign of welding irradiated Ni-base alloy 182 with refined laser parameters. Three coupons with doped boron concentration at 14, 15 and 23 wppm were used. Various laser welding parameters (weld speed, effective heat input, wire feed speed, with and without ABSI technique) were applied to study the influence on the formation of HeIC. To mitigate the crack issues in the weld toe region observed in the first weld campaign, the laser power of the entry pass of each layer was reduced from 1000W to 700W. Additional autogenous weld passes with 430W for low heat input condition and 660W for high heat input condition were conducted on each side of the weld toe regions. All welded samples are being cross-sectioned and characterized in more details. The results will be reported in the next fiscal year milestone report.

5. REFERNECES

Asano, K., S. Nishimura, Y. Saito, H. Sakamoto, Y. Yamada, T. Kato and T. Hashimoto (1999). "Weldability of neutron irradiated austenitic stainless steels." Journal of Nuclear Materials **264**(1-2): 1-9.

EPRI (2015). BWRVIP-97, Revision 1: BWR Vessel and Internals Project, Guidelines for Performing Weld Repairs to Irradiated BWR Internals, EPRI.

Feng, Z., R. G. Miller, N. Cetiner, X. Hu, S. Clark, G. Frederick and B. Sutton (2017). Report Summarizing the Status of Second Round Irradiation Experiments and Assessment of Materials Available for Testing Advanced Welding (M3LW-17OR0406013). DOE Light Water Reactor Sustainability Program, Oak Ridge National Laboratory.

Feng, Z., R. G. Miller, J. Chen, M. Gussev, X. Hu, W. Tang, G. Frederick, J. Tatman and B. Sutton (2019). Recent Technological Advances in Welding Irradiated Helium Containing Austenitic Steel (M3LW-19OR0406015). DOE Light Water Reactor Sustainability Program, Oak Ridge National Laboratory.

Feng, Z., R. G. Miller, J. Chen, W. Tang, S. Clark, B. Gibson, M. Vance, G. Frederick, J. Tatman and B. Sutton (2017). Development of Welding Parameters for Irradiated Materials (M2LW-17OR0406014). DOE Light Water Reactor Sustainability Program, Oak Ridge National Laboratory.

Feng, Z., W. Tang, R. G. Miller, J. Chen, S. Clark, B. Gibson, G. Frederick, J. Tatman and B. Sutton (2018). Complete Report on Development of Weld Repair Technology (M2LW-18OR0406014). DOE Light Water Reactor Sustainability Program, Oak Ridge National Laboratory.

Feng, Z., W. Tang, R. G. Miller, J. Chen, M. Gussev, S. Clark, G. Frederick, J. Tatman and B. Sutton (2019). Develop Parameters and Characterize the Quality of Friction Stir and Laser Weld-Repaired, Irradiated Structural Materials Representative of Extended Reactor Service Life (M2LW-19OR0406014). DOE Light Water Reactor Sustainability Program, Oak Ridge National Laboratory.

Feng, Z. and G. M. Wilkowski (2002). Repair Welding of Irradiated Materials - Modeling of Helium Bubble Distributions for Determining Crack-Free Welding Procedures. 10th International Conference on Nuclear Engineering, ASME.

Feng, Z., K. Wolfe and E. Willis (2009). BWRVIP-228: BWR Vessel and Internals Project: A Computational Modeling Tool for Welding Repair of Irradiated Materials, EPRI.

JNES (2004). FY2003 Nuclear Power Plant Maintenance Improvement Technology (PMT), Japan Nuclear Energy Safety Organization.

JNES (2004). FY2003 Safe Maintenance/Repair Welding Techniques for Nuclear Plant Irradiated Materails (WIM), Japan Nuclear Energy Safety Organization.

Kanne Jr., W. R. (1988). "Remote Reactor Repair, GTA weld cracking caused by entrapped helium." Welding Journal(8): 33-39.

Lin, H. T., M. L. Grossbeck and B. A. Chin (1990). "Cavity Microstructure and Kinetics During Gas Tungsten Arc Welding of Helium-Containing Stainless Steel." Metallurgical Transactions A **21A**(9): 2585-2596.

Willis, E. (2006). BWRVIP-151: BWR Vessle and Internals Project, Technical Basis for Resision to BWRVIP-97 Welding Guidelines, EPRI.